3,3′-Diindolylmethane Is a Novel Mitochondrial H^+-ATP Synthase Inhibitor that Can Induce $p21^{Cip1/Waf1}$ Expression by Induction of Oxidative Stress in Human Breast Cancer Cells

Yixuan Gong,[1] Heesook Sohn,[1] Ling Xue,[2] Gary L. Firestone,[2] and Leonard F. Bjeldanes[1]

Departments of [1]Nutritional Sciences and Toxicology and [2]Molecular and Cell Biology, University of California, Berkeley, California

Abstract

Epidemiologic evidence suggests that high dietary intake of *Brassica* vegetables, such as broccoli, cabbage, and Brussels sprouts, protects against tumorigenesis in multiple organs. 3,3′-Diindolylmethane, one of the active products derived from *Brassica* vegetables, is a promising antitumor agent. Previous studies in our laboratory showed that 3,3′-diindolylmethane induced a G_1 cell cycle arrest in human breast cancer MCF-7 cells by a mechanism that included increased expression of p21. In the present study, the upstream events leading to p21 overexpression were further investigated. We show for the first time that 3,3′-diindolylmethane is a strong mitochondrial H^+-ATPase inhibitor ($IC_{50} \sim 20$ μmol/L). 3,3′-Diindolylmethane treatment induced hyperpolarization of mitochondrial inner membrane, decreased cellular ATP level, and significantly stimulated mitochondrial reactive oxygen species (ROS) production. ROS production, in turn, led to the activation of stress-activated pathways involving p38 and c-Jun NH_2-terminal kinase. Using specific kinase inhibitors (SB203580 and SP600125), we showed the central role of p38 and c-Jun NH_2-terminal kinase (JNK) pathways in 3,3′-diindolylmethane-induced p21 mRNA transcription. In addition, antioxidants significantly attenuated 3,3′-diindolylmethane-induced activation of p38 and JNK and induction of p21, indicating that oxidative stress is the major trigger of these events. To further support the role of ROS in 3,3′-diindolylmethane-induced p21 overexpression, we showed that 3,3′-diindolylmethane failed to induce p21 overexpression in mitochondrial respiratory chain deficient ρ^0 MCF-7 cells, in which 3,3′-diindolylmethane did not stimulate ROS production. Thus, we have established the critical role of enhanced mitochondrial ROS release in 3,3′-diindolylmethane-induced p21 up-regulation in human breast cancer cells. (Cancer Res 2006; 66(9): 4880-7)

Introduction

3,3′-Diindolylmethane is a promising antitumor agent derived from *Brassica* food plants, including cabbage, broccoli, and Brussels, and other common dietary vegetables (1, 2). Several studies have shown that 3,3′-diindolylmethane can inhibit the development of both carcinogen-induced and implanted tumors in rodents (3, 4). In addition, 3,3′-diindolylmethane and its precursor indole-3-carbinol (I3C) are considered to be the preferred treatment for recurrent respiratory papillomatosis in humans (5).

Evidence is accumulating that 3,3′-diindolylmethane inhibits proliferation of cancer cells by inducing cell cycle arrest and apoptosis (4, 6–9). In previous studies of the cytostatic mode of action of 3,3′-diindolylmethane, we showed that this indole could cause a G_1 cell cycle arrest regardless of estrogen receptor or p53 tumor suppressor status of breast tumor cells (8). Analysis of G_1-acting cell cycle components indicated that the enzymatic activity of cyclin-dependent kinase 2 (CDK2) was strongly reduced by 3,3′-diindolylmethane by a mechanism that involved a large increase in expression of the CDK inhibitor, $p21^{cip1/waf1}$ (p21). $p21^{Cip1/Waf1}$ is a well-characterized Cip/Kip family CDK inhibitor, which can induce G_1 arrest and block entry into S phase by inactivating CDKs or by inhibiting activity of proliferating cell nuclear antigen (10). Further promoter deletion analysis of the p21 promoter showed that 3,3′-diindolylmethane responsiveness was partially dependent on the binding of the Sp1 and Sp3 transcription factors to the GC-rich region of the proximal promoter.

Our previous studies also showed that 3,3′-diindolylmethane strongly induced the stress-activated protein kinase pathways, c-Jun NH_2-terminal kinase (JNK) and p38, in human breast cancer MCF-7 cells, which contribute to 3,3′-diindolylmethane-induced IFN-γ expression (11). JNK and p38 kinases are important in controlling cell growth and apoptosis in response to chemical stress, radiation, and growth factors (12). The involvement of JNK and p38 activation in 3,3′-diindolylmethane-induced p21 expression in MCF-7 cells has not been reported.

Results of our most recent studies have shown that high concentrations of 3,3′-diindolylmethane (≥75 μmol/L) can induce a G_2 cell cycle arrest in human hepatoma cells by a mechanism that involves induction of cellular oxidative stress and activation of DNA damage checkpoint signaling pathways.[3] Because oxidative stress has been shown to activate p21 expression in other systems (13, 14), we sought to determine whether reactive oxygen species (ROS) might contribute to the mechanism of increased p21 expression by 3,3′-diindolylmethane in breast tumor cells. Here, we show that 3,3′-diindolylmethane could strongly enhance mitochondrial ROS release by inhibition of mitochondrial H^+-ATPase, leading to activation of the p38 and JNK stress pathways and up-regulation of cell cycle inhibitor p21 expression.

Materials and Methods

Chemicals. All the cell culture reagents except fetal bovine serum (Omega Scientific, Inc., Tarzana, CA) were from Life Technologies/Invitrogen (Carlsbad, CA). 3,3′-Diindolylmethane was purchased from LKT Laboratory, Inc. (St. Paul, MN). RNase, propidium iodide, α-tocopherol,

Requests for reprints: Leonard F. Bjeldanes, Department of Nutritional Sciences and Toxicology, 119 Morgan Hall, University of California, Berkeley, CA 94720-3104. Phone: 510-642-1601; Fax: 510-642-0535; E-mail: lfb@nature.berkeley.edu.

©2006 American Association for Cancer Research.

doi:10.1158/0008-5472.CAN-05-4162

[3] Y. Gong, G.L. Firestone, and L.F. Bjeldanes, unpublished data.

Downloaded from cancerres.aacrjournals.org on March 25, 2019. © 2006 American Association for Cancer Research.

ascorbic acid, antimycin A, oligomycin, digitonin, ATP, NADH, phosphoenolpyruvate (PEP), pyruvate kinase (PK), lactate dehydrogenase (LDH), succinate, phenylmethylsulfonyl fluoride (PMSF), DTT, leupeptin, aprotinin, pepstatin, β-glycerophosphate, sodium fluoride, sodium orthovanadate, and glutathione assay kit were from Sigma (St. Louis, MO). Rhodamine 123, CM-H_2DCFDA, and tetramethylrhodamine, methyl ester, perchlorate (TMRM) were purchased from Molecular Probes (Eugene, OR). SB203580 and SP600125 were from Calbiochem (San Diego, CA). ENLITEN rLuciferase/Luciferin Reagent was a product of Promega (Madison, WI). All other reagents were of the highest grade available.

The antibody against p21 was from Oncogene Research Products (San Diego, CA). The antibody against β-tubulin was from Santa Cruz Biotechnology (Santa Cruz, CA). The antibodies against p-p38, p-INK, p-retinoblastoma (pRb), p38, JNK, and Rb were all purchased from Cell Signal Technology (Beverly, MA).

Cell culture and generation of mitochondrial DNA-deficient cells. The human mammary carcinoma MCF-7 and MDA-MB-231 cell lines were obtained from the American Type Culture Collection (Manassas, VA). Cells were cultured in 10-cm Petri dishes in DMEM supplemented with 10% fetal bovine serum, 100 units/mL penicillin, and 100 units/mL streptomycin in a humidified incubator with 5% CO_2 at 37°C. MCF-7 cells lacking mitochondrial DNA (mtDNA; ρ^0) were generated as described previously by growing MCF-7 cells in DMEM supplemented with 10% fetal bovine serum, 1 mmol/L pyruvate, 50 μg/mL uridine, and 50 ng/mL ethidium bromide for 8 weeks (15). The absence of mtDNA was confirmed by PCR analysis using the following specific mtDNA primers (16): mtDNA-1, 5′-CCTAGGGATAACAGCGCAAT-3′; mtDNA-2, 5′-TAGAAGAGCGATGGTGAGAG-3′.

Western blot. Cells were scraped from 10-cm Petri dishes, washed twice with PBS, and then suspended in 1 mL of radioimmunoprecipitation assay buffer containing 50 mmol/L Tris-HCl (pH 7.5), 150 mmol/L NaCl, 1% NP40, 0.1% SDS, 1 mmol/L NaF, 100 μg/mL PMSF, 1 mmol/L DTT, 2 μg/mL leupeptin, 2 μg/mL aprotinin, 1 μg/mL pepstatin, 10 mmol/L β-glycerophosphate, and 1 mmol/L sodium orthovanadate on ice for 30 minutes. After centrifugation at 13,200 rpm for 15 minutes at 4°C, the supernatants were collected, and the proteins were separated on either 12% or 15% SDS-PAGE. After electrophoresis, proteins were transferred to an Immobilon-P membrane (Millipore, Bedford, MA). The membrane was blocked with 5% nonfat milk or bovine serum albumin in TBST and incubated overnight with the corresponding primary antibodies at 4°C. After washing thrice with TBST, the membrane was incubated at room temperature for 1 hour with horseradish peroxidase–conjugated secondary antibody diluted with TBST (1:1,000). The detected protein signals were visualized by an enhanced chemiluminescence reaction system (Amersham, Arlington Heights, IL).

Reverse transcription-PCR. Total RNA was extracted using TRIzol reagent as recommended by the manufacturer (Invitrogen). cDNA was prepared from 5 μg of total RNA by reverse transcription in a volume of 50 μL with superscript reverse transcriptase (Invitrogen). The resultant cDNA was subjected to PCR (94°C for 45 seconds, 57°C for 1 minute, and 72°C for 1.5 minutes) using specific primers synthesized by Genosys (Woodlands, TX) in a Robocycler Gradient 96 (Stratagene, La Jolla, CA). PCR fragments were analyzed on 1% agarose/TAE gels. Primer sequences for PCR amplification are as follows: p21-1, 5′-CAGGTCCACATGGTCTTCCT-3′; p21-2, 5′-CTGCCCAAGCTCTACCTTCC-3′; glyceraldehyde-3-phosphate dehydrogenase (GAPDH)-1, 5′-ACCACAGTCCATGCCATCAC-3′; GAPDH-2, 5′-TCCACCACCCTGTTGCTGTA-3′.

Measurement of mitochondrial membrane potential. Cells were seeded into six-well culture plates at a density of 5×10^5/mL, and 24 hours later, they were treated with different concentrations of 3,3′-diindolylmethane or 5 μmol/L carbonyl cyanide 4-(trifluoromethoxy)phenylhydrazone (FCCP; proton gradient uncoupler) for 1 hour. During the last 30 minutes of treatment, either rhodamine 123 (100 nmol/L) or TMRM (40 nmol/L) was added to the medium to measure the mitochondrial membrane potential (MMP). Cells were collected by gentle trypsinization and analyzed on a Beckman-Coulter EPICS XL flow cytometer, and data were processed by WinMDI 2.8 software.

Measurement of ROS production in whole cells and in isolated mitochondria. Intracellular ROS were detected with the cell permeable fluorescent probe CM-H_2DCFDA. MCF-7 cells were seeded into six-well culture plates at a density of 5×10^5/mL, and 24 hours later, they were treated with different concentrations of 3,3′-diindolylmethane for 1 hour in the presence or the absence of antioxidants. During the last 30 minutes of treatment, cells were loaded with 1 μg/mL CM-H_2DCFDA for 30 minutes in the dark at 37°C. Cells were then trypsinized and analyzed on a Beckman-Coulter EPICS XL flow cytometer. Data were processed by WinMDI 2.8 software.

Mitochondria were isolated from cultured MCF-7 cells by differential centrifugation according to the Pierce mitochondria isolation kit manual (Rockford, IL). To analyze the mitochondrial ROS production, isolated mitochondria were suspended in 500 μL analysis buffer [250 mmol/L sucrose, 20 mmol/L 3-(*N*-morpholino) butane sulfonic acid, 10 mmol/L Tris-base, 100 μmol/L KH_2PO_4, 0.5 mmol/L Mg^{2+}, 1 μmol/L cyclosporin A (pH 7.0)] containing 5 mmol/L succinate and 1 μg/mL CM-H_2DCFDA (17). In some samples, antimycin A (an inhibitor of complex III; 2.5 μg/mL) was added to enhance ROS production. Mitochondria suspension were incubated at room temperature, protected from light for 30 minutes and then analyzed by Beckman-Coulter EPICS XL flow cytometer. Data were processed with WinMDI 2.8 software.

Measurement of cellular ATP and GSH levels. For ATP content analysis, cells were seeded in six-well plates at a density of 5×10^5/mL and treated with different concentrations of drugs for the indicated times. Cells were washed with cold PBS twice and lysed in a solution containing 0.5% trichloroacetic acid and 4 mmol/L EDTA. The supernatants obtained following a 5-minute spin at 13,000 rpm were diluted 50× with distilled water for bioluminescent ATP content measurement using Promega ENLITEN rLuciferase/Luciferin reagent as instructed by the manufacturer.

For GSH content analysis, cells were seeded in a 10-cm Petri dish at a density of 5×10^6/mL and treated with different concentrations of drugs for the indicated times. The intracellular GSH levels were measured by GSH kit from Sigma.

PK/LDH–coupled ATPase assay. Fresh isolated mitochondria were solubilized in 1% digitonin solubilizing buffer containing 50 mmol/L Tris-HCl (pH 7.4), 120 mmol/L NaCl, 5 mmol/L KCl, 1 mmol/L $MgSO_4$, 1 mmol/L $CaCl_2$, and 10% glycerol for 30 minutes at 4°C. The ATPase activity of solubilized mitochondria was measured spectrophotometrically at 340 nm by coupling the production of ADP to the oxidation of NADH via pyruvate kinase and lactate dehydrogenase as described previously (18). The reaction mixture contained a final volume of 400 μL at 25°C and included the following: Tris-HCl (pH 8), 2 mmol/L ATP, 2 mmol/L $MgCl_2$, 50 mmol/L KCl, 0.2 mmol/L EDTA, 0.2 mmol/L NADH, 1 mmol/L PEP, 5 units pyruvate kinase, 8 units lactate dehydrogenase, and 25 to 50 μg mitochondrial proteins. These assay conditions minimized the contribution of other transport ATPases, such as Na^+,K^+-ATPase. Test compounds were added before the reaction was started by addition of 25 to 50 μg of solubilized mitochondria at a constant temperature of 25°C.

Statistical analysis. The statistical differences between groups were determined using Student's *t* test. The levels of significance are noted for $P < 0.01$ and $P < 0.05$. The results are expressed as means ± SD for at least three replicate determinations for each assay.

Results

3,3′-Diindolylmethane increased MMP in both MCF-7 and MDA-MB-231 cells. We reported previously that 3,3′-diindolylmethane induced apoptosis in human breast cancer cells (8). Because depolarization of the mitochondrial membrane is established to be part of the mitochondria-mediated apoptotic pathway (19), we examined MMP in 3,3′-diindolylmethane-treated MCF-7 cells using rhodamine 123 and TMRM dyes. These cell-permeable fluorescent probes are actively sequestered by mitochondria according to the membrane potential without causing cytotoxic effects. Surprisingly, the flow cytometry results for both

Downloaded from cancerres.aacrjournals.org on March 25, 2019. © 2006 American Association for Cancer Research.

probes presented in Fig. 1*A* show that 3,3′-diindolylmethane concentration-dependently increased MMP 1 hour after treatment in MCF-7 cells. 3,3′-Diindolylmethane (50 μmol/L) almost doubled the fluorescence intensity, indicating a hyperpolarization of the mitochondrial membrane. FCCP, a mitochondrial proton gradient dissipater, showed the opposite effect by decreasing MMP. Similar effects were observed in MDA-MB-231 breast cancer cells after 3,3′-diindolylmethane or FCCP treatment (data not shown). Results presented in Fig. 1*B* show that after 24 hours of 3,3′-diindolylmethane treatment, most cells displayed depolarized MMP. Thus, 3,3′-diindolylmethane induced a biphasic change in MMP that involved a concentration-dependent increase within the first hour of treatment followed by a reduction after 24 hours of treatment.

3,3′-Diindolylmethane inhibited mitochondrial H^+-ATPase. MMP results from a proton gradient established during the electron transport, which is used by mitochondrial H^+-ATP synthase to produce ATP. Inhibition of the mitochondrial H^+-ATP synthase by drugs, such as oligomycin, often results in an increase in MMP (20, 21) Thus, we examined whether 3,3′-diindolylmethane could inhibit mitochondrial ATP synthase.

Mitochondrial H^+-ATP synthase (H^+-ATPase) can catalyze both ATP synthesis and ATP hydrolysis. When there is a proton gradient, the enzyme catalyzes the forward reaction (ATP synthesis), and when there is no gradient, it displays H^+-ATPase activity (22). The effect of 3,3′-diindolylmethane on mitochondrial H^+-ATPase activity was determined using 1% digitonin-solubilized, freshly isolated mitochondria from both MCF-7 cells and mouse liver. Data presented in Fig. 2*A* show that 3,3′-diindolylmethane concentration-dependently inhibited H^+-ATPase activity in mitochondria extracted from MCF-7 cells, with IC_{50} of ~20 μmol/L. Similar levels of inhibition were seen in mitochondria extracted from mouse liver (data not shown). I3C, the precursor of

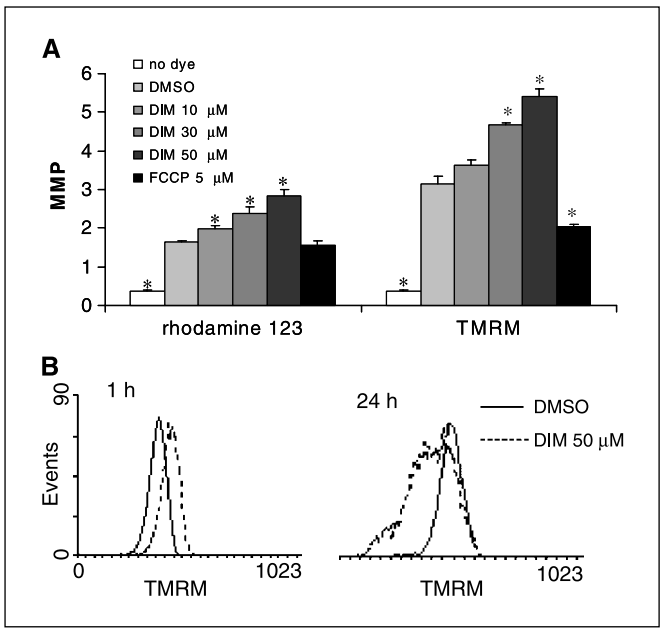

Figure 1. 3,3′-Diindolylmethane (*DIM*) induced a transient increase in MMP in MCF-7 cells. *A,* 3,3′-diindolylmethane induced mitochondrial membrane hyperpolarization in MCF-7 cells. MCF-7 cells were treated with different concentrations of 3,3′-diindolylmethane for 1 hour, and during the last 30 minutes of treatment, either rhodamine 123 (100 nmol/L) or TMRM (40 nmol/L) was added to the medium to measure MMP. Cells were then analyzed by Beckman-Coulter EPICS XL flow cytometer. *Columns,* mean fluorescence intensity; *bars,* SD. *B,* comparison of MMP by TMRM staining in MCF-7 cells after 1 and 24 hours of 50 μmol/L 3,3′-diindolylmethane treatment. The original flow cytometry data were processed by WinMDI 2.8 software. *, $P < 0.01$, significant differences compared with control.

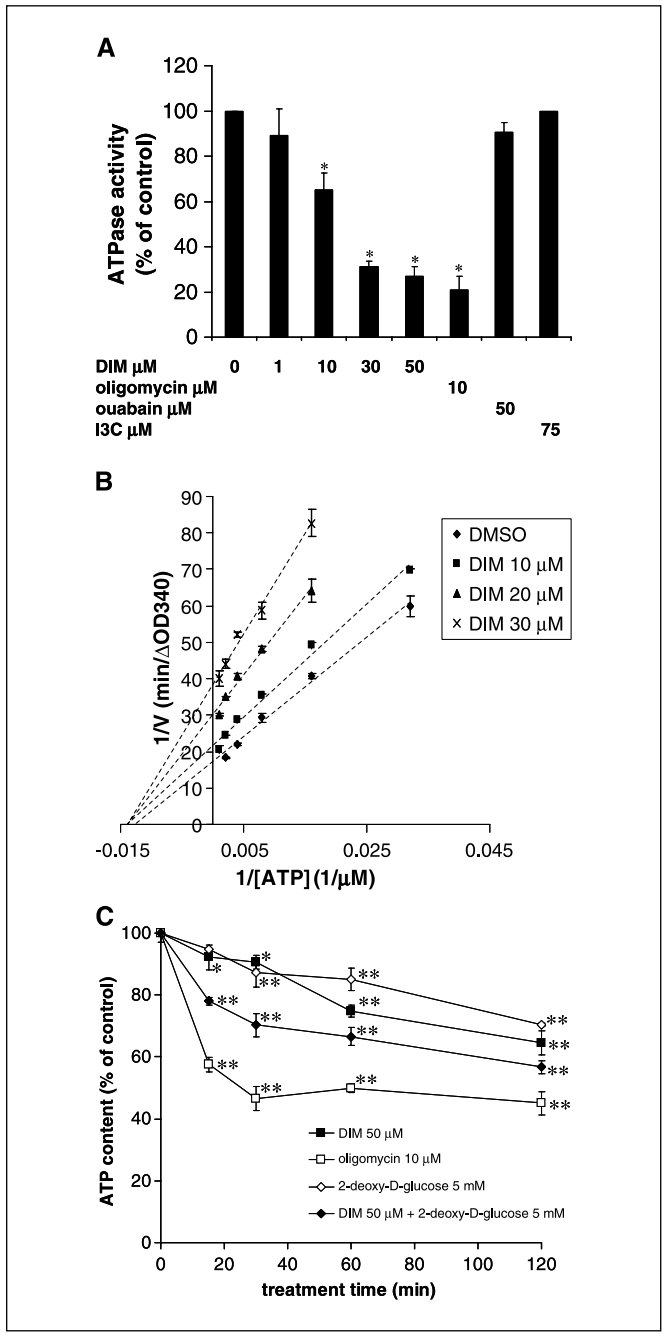

Figure 2. 3,3′-Diindolylmethane (*DIM*) noncompetitively inhibited mitochondiral H^+-ATPase activity. *A,* 3,3′-diindolylmethane inhibited H^+-ATPase activity in 1% digitonin-solubilized mitochondria isolated from MCF-7 cells. The preparation of mitochondria and PK/LDH–coupled ATPase assay was described in Materials and Methods. *B,* double reciprocal plot analysis of the inhibition of mouse liver mitochondrial H^+-ATPase by 3,3′-diindolylmethane. *, $P < 0.01$, significant differences compared with control. *C,* 3,3′-diindolylmethane depleted intracellular ATP. MCF-7 cells were seeded in low glucose medium and treated with different ATP-depleting drugs for the indicated times. The intracellular ATP concentration was measured by ENLITEN rLuciferase/Luciferin Reagent from Promega as described in Materials and Methods. The ATP concentration of untreated cells was set as 100%. *, $P < 0.05$, significant differences compared with untreated cells.

Downloaded from cancerres.aacrjournals.org on March 25, 2019. © 2006 American Association for Cancer Research.

3,3′-diindolylmethane in plants, showed no effect on enzyme activity. The extent of inhibition by 3,3′-diindolylmethane (50 μmol/L) was comparable with the effect of the well-known H^+-ATPase inhibitor, oligomycin (10 μmol/L). Ouabain, a selective Na^+,K^+-ATPase inhibitor, produced no significant effect on the total H^+-ATPase activity, indicating Na^+,K^+-ATPase activity did not significantly interfere with our reaction.

The inhibitory effects of 3,3′-diindolylmethane on mouse liver mitochondrial H^+-ATPase activity are summarized in the double reciprocal plot shown in Fig. 2*B* and indicate that 3,3′-diindolylmethane is a noncompetitive inhibitor of mitochondrial H^+-ATPase.

3,3′-Diindolylmethane decreased ATP levels in MCF-7 cells. 3,3′-Diindolylmethane-mediated mitochondrial H^+-ATPase inhibition was further confirmed by determination of a change in cellular ATP level. The results presented in Fig. 2*C* show that 3,3′-diindolylmethane (50 μmol/L) time-dependently decreased cellular ATP level by 15 minutes after treatment. By 2 hours, the level of intracellular ATP had dropped by 36%. A greater and more rapid decrease to a maximum of 55% inhibition was observed in the positive control oligomycin-treated cells. 2-Deoxy-D-glucose (5 mmol/L), a glycolytic pathway competitive inhibitor (23), decreased ATP concentration by 30% after a 2-hour treatment. Because the glycolytic pathway and mitochondrial oxidative phosphorylation are the two major cellular ATP-generating pathways, we also measured the effects of cotreatment with 3,3′-diindolylmethane and 2-deoxy-D-glucose on cellular ATP levels. The results indicated that the combination produced a roughly additive decrease in cellular ATP level, especially at the early time points.

3,3′-Diindolylmethane induced mitochondrial ROS production. Release of ROS in the form of superoxide anion occurs normally during oxidative phosphorylation to the extent of about 3% to 5% of total oxygen consumed (24). This rate of ROS production can be increased greatly, however, under certain conditions when oxidative phosphorylation is inhibited by drugs (20, 25–27). To determine whether 3,3′-diindolylmethane functions in a similar manner, we examined the effect of 3,3′-diindolylmethane on cellular ROS levels using the ROS-sensitive dye CM-H_2DCFDA. Our results indicate that 3,3′-diindolylmethane (50 μmol/L) clearly increased the level of cellular ROS, as did hydrogen peroxide and the other oxidative phosphorylation inhibitors oligomycin and antimycin A (data not shown). The ROS production occurred within 5 minutes of 3,3′-diindolylmethane treatment, and their levels were reduced on coincubation with antioxidants (shown in Fig. 3*A*). The results presented in Fig. 3*B* indicate that the induction of ROS occurred in a clear 3,3′-diindolylmethane concentration-dependent manner with 30 μmol/L, the apparent threshold for the activity in the cells. To confirm that the 3,3′-diindolylmethane-mediated ROS release produces an oxidative stress on the cells, Fig. 3*C* illustrates the effects of 3,3′-diindolylmethane on intracellular glutathione levels. The results indicate that the positive control, hydrogen peroxide, and 3,3′-diindolylmethane treatment caused similar 40% and 50% decreases, respectively, in total glutathione level.

To further verify the role of mitochondria in the 3,3′-diindolylmethane-induced oxidative burst, we directly treated mitochondria freshly isolated from MCF-7 cells with different concentrations of 3,3′-diindolylmethane and examined the ROS production over time. The results presented in Fig. 3*D* indicate that antimycin A (10 μmol/L), a mitochondrial complex III inhibitor, significantly stimulated mitochondrial ROS production, as did 3,3′-diindolylmethane in a concentration-dependent manner. Taken together, these results show that 3,3′-diindolylmethane treatment caused oxidative stress in cells through stimulating ROS release from mitochondria.

3,3′-Diindolylmethane induced p21 upregulation through oxidative stress. We reported previously that 3,3′-diindolylmethane induced a G_1 cell cycle arrest in MCF-7 cells that was accompanied by a strong increase in the expression of the cell cycle inhibitor p21 (8). Here, we examined the role of oxidative stress in 3,3′-diindolylmethane-induced p21 expression. Control experiments confirmed that hydrogen peroxide treatment increased p21 expression in MCF-7 cells (data not shown). Results of Western blot analysis showed that 3,3′-diindolylmethane concentration-dependently increased p21 expression in MCF-7 cells, which could be abolished by antioxidants (Fig. 4*A* and *B*).

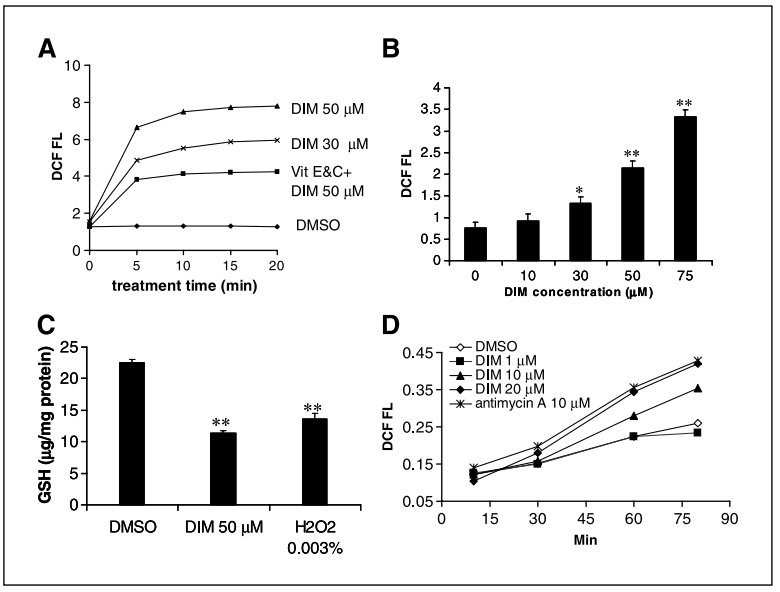

Figure 3. 3,3′-Diindolylmethane (*DIM*) induced ROS production from mitochondria. *A,* 3,3′-diindolylmethane treatment rapidly induced ROS release in MCF-7 cells, and the effects were partially reversed with reducing agents. DCF fluorescence was recorded by flow cytometer immediately after 3,3′-diindolylmethane addition in MCF-7 cells preloaded with 1 μg/mL CM-H_2DCFDA for 30 minutes. *Points,* mean fluorescence intensity; *bars,* SD. *B,* 3,3′-diindolylmethane concentration-dependently increased ROS release in MCF-7 cells after 1 hour of treatment. *C,* 3,3′-diindolylmethane-induced oxidative stress decreased cellular antioxidant glutathione after 24 hours of treatment as measured by Sigma glutathione assay kit. *D,* 3,3′-diindolylmethane directly stimulated ROS release in freshly isolated mitochondria as shown by flow cytometry analysis. The isolation of mitochondria and assay procedures are described in Materials and Methods. Antimycin A, a known mitochondrial ROS inducer, was used as a positive control. *, $P < 0.05$, significant differences compared with control. **, $P < 0.01$, significant differences compared with control.

Downloaded from cancerres.aacrjournals.org on March 25, 2019. © 2006 American Association for Cancer Research.

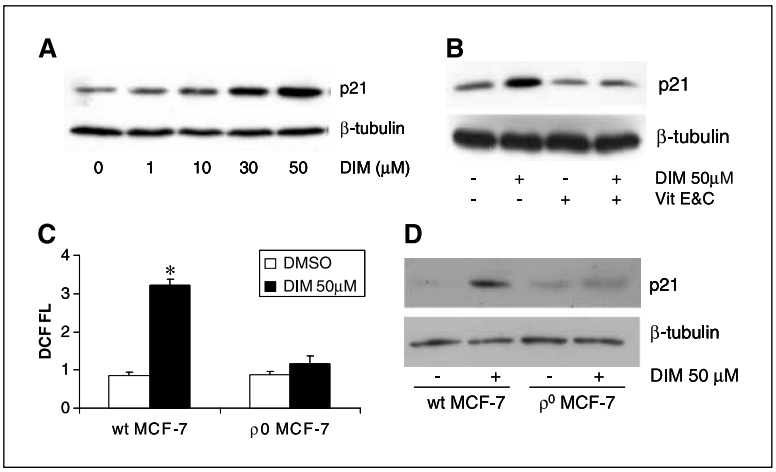

Figure 4. 3,3′-Diindolylmethane (*DIM*)–induced oxidative stress contributed to p21 overexpression. *A,* 3,3′-diindolylmethane treatment induced p21 overexpression shown by Western blot analysis. MCF-7 cells were treated with different concentrations of 3,3′-diindolylmethane for 24 hours. Western blot analysis was done as described in Materials and methods. β-Tubulin serves as an internal loading control. *B,* the combination of vitamin E (300 μM) and C (500 μM) prevented 3,3′-diindolylmethane-induced p21 overexpression shown by Western blot analysis. *C,* ρ^0 MCF-7 cells have significantly lower ROS production after 3,3′-diindolylmethane stimulation. *D,* 3,3′-diindolylmethane failed to induce p21 overexpression in ρ^0 MCF-7 cells as shown by Western blot analysis. *, $P < 0.05$, significant differences compared with untreated cells.

To further test our hypothesis, we examined the effects of 3,3′-diindolylmethane on ROS releases and p21 expression in ρ^0 MCF-7 cells, which are mtDNA-deficient cells and are not capable of carrying out oxidative phosphorylation (15). Reverse transcription-PCR (RT-PCR) analysis showed that mtDNA content was decreased by >95% in the ρ^0 MCF-7 cells (data not shown). Results presented in Fig. 4*C* and *D* show that whereas 3,3′-diindolylmethane (50 μmol/L) treatment produced ~4-fold increase in ROS-associated fluorescence in wild-type MCF-7 cells, this indole did not significantly elevate ROS levels or increase p21 expression in ρ^0 MCF-7 cells. Taken together, these results support the hypothesis that 3,3′-diindolylmethane can induce p21 expression in MCF-7 cells by enhancing ROS release from mitochondria.

3,3′-Diindolylmethane-induced ROS release resulted in pRb inactivation by activation of JNK and p38 stress-activated pathways. We next examined the effect of 3,3′-diindolylmethane-induced oxidative stress on upstream and downstream signaling events associated with p21 expression and cell cycle arrest. We found in a recent study that high concentrations of 3,3′-diindolylmethane (≥75 μmol/L) could induce oxidative DNA damage and activate the DNA checkpoint 2 pathway in human hepatoma cells, thus leading to G_2 cell cycle arrest. In this study, lower concentrations of 3,3′-diindolylmethane (≤50 μmol/L) were used to avoid DNA damage–induced signaling pathways. JNK and p38 signaling pathways are well established as mediators of stress-induced cell cycle arrest and apoptosis (28), and both pathways were activated by 3,3′-diindolylmethane in our previous study (11, 29–31). Here, we investigated the involvement of these two pathways in 3,3′-diindolylmethane-induced p21 expression. Results presented in Fig. 5 show that these stress pathways were activated by 3,3′-diindolylmethane by a mechanism that was blocked by antioxidants and which resulted in p21 expression and Rb hypophosphorylation. Thus, results of Western blot analysis presented in Fig. 5*A* show that 3,3′-diindolylmethane treatment produced a rapid and persistent increase in phosphorylation of both JNK (p54 and p46 isoforms) and p38 kinases. The results presented in Fig. 5*B* indicate that the 3,3′-diindolylmethane-induced phosphorylation of JNK and p38 were strongly reduced by cotreatment with antioxidants. Furthermore, inhibitors of JNK kinase (SP600125) and of p38 kinase (SB203580), which, respectively, prevented JNK and p38 phosphorylation (see Fig. 5*C*), effectively inhibited the 3,3′ -diindolylmethane-induced increase in p21 mRNA level, as shown by the results of RT-PCR analysis presented in Fig. 5*D*. Results of Western blot analysis presented in Fig. 5*E* show that 3,3′-diindolylmethane strongly induced Rb dephosphorylation and thus activated this tumor suppressor. The specific JNK and p38 kinase inhibitors blocked both the inducing effect of this indole on p21 expression and partially reversed the inhibitory effect of 3,3′-diindolylmethane on Rb phosphorylation. Taken together, these results confirm that 3,3′-diindolylmethane can increase p21 expression by a mechanism that involves ROS-mediated activation of JNK and p38 kinases and results in hypophosphorylation and activation of Rb protein.

Discussion

We have previously published that 3,3′-diindolylmethane could induce a G_1 cell cycle arrest in human breast cancer MCF-7 cells that was associated with strong induction of cell cycle inhibitor, p21 (8). As summarized in Fig. 6, we now further report that 3,3′-diindolylmethane is a potent mitochondrial H^+-ATPase inhibitor (IC_{50} ~ 20 μmol/L). 3,3′-Diindolylmethane not only induced mitochondrial membrane hyperpolarizaton and reduced intracellular [ATP], but also enhanced mitochondrial ROS release, which led to the activation of stress-sensitive JNK and p38 pathways and increased expression of p21. These effects were not produced by 3,3′-diindolylmethane in mitochondrial respiratory chain deficient ρ^0 MCF-7 cells, thus indicating the essential role of mitochondria in the induction of p21 expression by 3,3′-diindolylmethane in human breast tumor cells. We have shown previously that the activation of p38 and JNK pathways was also responsible for 3,3′-diindolylmethane-induced IFN-γ secretion in MCF-7 cells (11). Now by showing that antioxidants prevented the activation of these two pathways, we further conclude that 3,3′-diindolylmethane-enhanced mitochondrial ROS release is the upstream signaling event leading to the induced IFN-γ expression.

Results of our double-reciprocal analysis establish that 3,3′-diindolylmethane is a direct, noncompetitive inhibitor of mitochondrial H^+-ATPase. This activity is particularly promising for the development of 3,3′-diindolylmethane as a therapeutic agent because a family of H^+-ATPase inhibitors, including oligomycin, was shown recently to be among the most cell line selective cytostatic agents of 37,000 substances tested against the 60 human cancer cell lines of the National Cancer Institute (32). Our previous studies revealed that both cell cycle arrest and apoptosis contributed to 3,3′-diindolylmethane-induced cytostatic effects in

Downloaded from cancerres.aacrjournals.org on March 25, 2019. © 2006 American Association for Cancer Research.

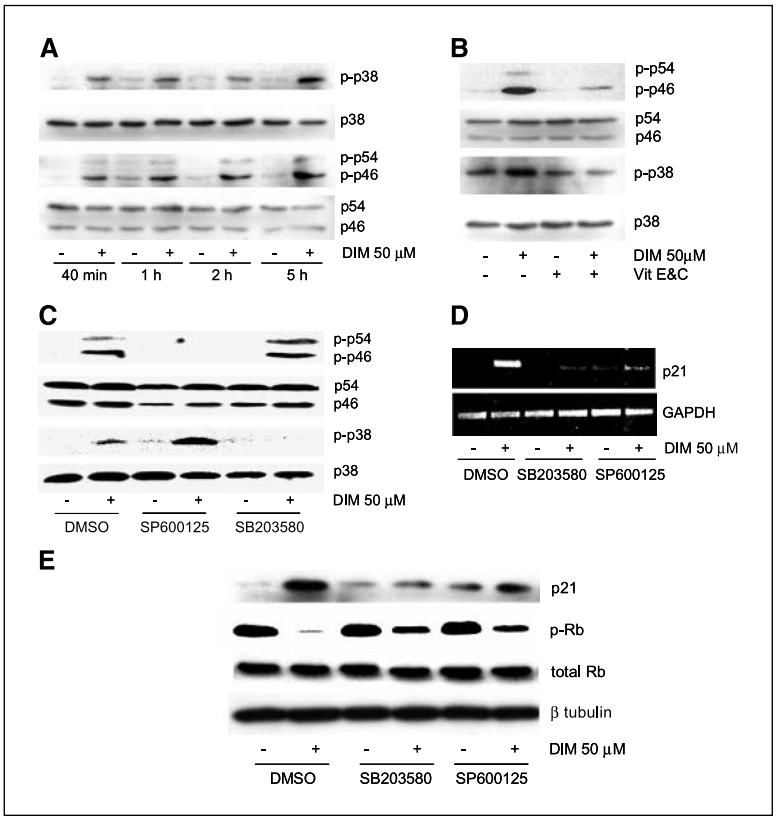

Figure 5. JNK and p38 pathways mediated 3,3′-diindolylmethane (*DIM*)–induced p21 overexpression. *A,* MCF-7 cells were treated with 3,3′-diindolylmethane (50 μmol/L) or vehicle DMSO for the indicated times, and Western blot was done as described in Materials and Methods. *B,* cotreatment with vitamins E and C prevented 3,3′-diindolylmethane-induced p38 and JNK phosphorylation as shown by Western blot analysis. *C,* pharmacologic inhibitors of JNK and p38 kinases prevented 3,3′-diindolylmethane-induced JNK and p38 phosphorylation as shown by Western blot analysis. MCF-7 cells were pretreated with 20 μmol/L SB203580 (p38 inhibitor) or 8 μmol/L SP600125 (JNK inhibitor) for 30 minutes before 1 hour of 3,3′-diindolylmethane treatment. *D,* pharmacologic inhibitors of JNK and p38 kinases prevented 3,3′-diindolylmethane-induced p21 mRNA up-regulation as shown by RT-PCR analysis. MCF-7 cells were pretreated with 20 μmol/L SB203580 (p38 inhibitor) or 8 μmol/L SP600125 (JNK inhibitor) for 30 minutes before 24 hours of 3,3′-diindolylmethane treatment. *E,* SB203580 and SP600125 prevented 3,3′-diindolylmethane-induced p21 overexpression at the protein level and reversed 3,3′-diindolylmethane-induced Rb hypophosphorylation as shown by Western blot analysis.

MCF-7 cells (8, 9). The identification of 3,3′-diindolylmethane as a mitochondrial H^+-ATPase inhibitor may explain the cytostatic effects of 3,3′-diindolylmethane.

We have shown that 2 hours of 3,3′-diindolylmethane treatment depleted the cellular ATP levels by one third. ATP is the major readily useable form of energy involved in many crucial cellular processes. It is known that if cells fail to coordinate energy-supply and energy-consumption, they either arrest or initiate apoptosis to avoid possible replication errors (33, 34). Inhibitors of oxidative phosphorylation, which decrease the intracellular ATP concentration, induce cell cycle arrest and apoptosis in various types of tumor cells (34–36). Thus, by lowering intracellular ATP level, 3,3′-diindolylmethane imposes cytostatic restraints in fast-growing tumor cells.

We have shown further that enhanced mitochondrial ROS release by 3,3′-diindolylmethane leads to increased expression of the important cell cycle inhibitor p21, contributing to 3,3′-diindolylmethane-induced G_1-S arrest. ROS are well-known regulators of cell cycle progression and apoptosis (24, 37–39). We observed that depending on the concentration, 3,3′-diindolylmethane could rapidly induce ROS production in all the cell lines that we examined, including human breast cancer cells, prostate cancer cells, hepatoma cells, leukemia cells, and primary endothelial cells (data not shown). Induction of p21 through a p53-independent pathway is quite common in ROS-induced cell cycle arrest (14, 40–42). These p53-independent pathways activate the binding of the Sp1 family of transcription factors to the six Sp1-binding sites located in the proximal promoter of p21. Mitogen-activated protein kinase pathway components, especially c-*jun*, which are subject to redox control (29–31), can transactivate the promoter of human p21 by acting as a superactivator of Sp1 (43). Thus, our observations that 3,3′-diindolylmethane could produce ROS-dependent and p38 and JNK-mediated induction of p21 are consistent with our previous findings that 3,3′-diindolylmethane induced p21 expression through a p53-independent and Sp1-dependent pathway (8).

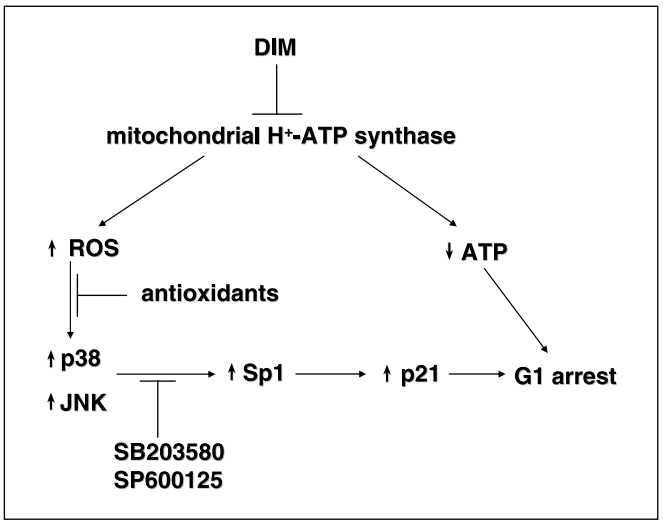

Figure 6. Proposed model for 3,3′-diindolylmethane (*DIM*)–induced p21 expression and G_1 cell cycle arrest. 3,3′-Diindolylmethane is a novel mitochondrial H^+-ATP synthase inhibitor. Like many other mitochondrial oxidative phosphorylation inhibitors, 3,3′-diindolylmethane treatment decreases cellular ATP level and increases mitochondrial ROS release. The latter then leads to activation of the redox-sensitive JNK and p38 pathway, which can be reversed by treatment with antioxidants. Activated JNK and p38 pathways will induce p21 transcription through activation of transcriptional factors, such as Sp1. Up-regulation of p21 and inhibition of ATP synthesis may both contribute to 3,3′-diindolylmethane-induced G_1 cell cycle arrest.

Downloaded from cancerres.aacrjournals.org on March 25, 2019. © 2006 American Association for Cancer Research.

Both of the above two mechanisms (ATP depletion and ROS production) seem involved in 3,3′-diindolylmethane-induced cytostatic effects. Antioxidants could block ROS generation and induction of p21, but they could not completely reverse 3,3′-diindolylmethane-induced G_1 cell cycle arrest or the 3,3′-diindolylmethane-induced inhibition of DNA synthesis (data not shown). This partial effect of antioxidants on reversing the antiproliferative activities of 3,3′-diindolylmethane suggests that both of the above mechanisms are important for 3,3′-diindolylmethane-induced cytostatic effects.

3,3′-Diindolylmethane induced a biphasic change in MMP that involved an increase within the first hour of treatment followed by a reduction after 24 hours of treatment (see Fig. 1). Because the alterations in mitochondrial structure and function play key roles in the regulation of apoptosis, both mitochondrial depolarization and hyperpolarization have been recognized as early events in apoptosis (44, 45). Thus, 3,3′-diindolylmethane-induced alterations in mitochondrial membrane integrity could contribute to 3,3′-diindolylmethane-induced apoptosis. However, the direct involvement of alteration of mitochondrial membrane integrity in p21 expression and cell cycle arrest has not yet been defined.

The bulk of our current studies were done at a 50 μmol/L concentration of 3,3′-diindolylmethane, at which p21 was highly induced; however, only minimal (up to 15%) apoptosis was seen (9). It is noteworthy that the roles of p21 induction in cell cycle arrest and apoptosis are different. Whereas p21 plays a crucial rule in inducing cell cycle arrest, p21 may act as a major inhibitor of both p53-dependent or p53-independent apoptosis (46). It is possible that the inhibitory effect of p21 on apoptosis might account for the low amount of apoptosis observed at this concentration of 3,3′-diindolylmethane.

Our data indicate that 3,3′-diindolylmethane is a potent mitochondrial H^+-ATPase inhibitor that can decrease cellular ATP levels, induce mitochondrial ROS release, activate stress-responsive p38 and JNK pathways, and up-regulate p21 expression in human breast cancer cells. Our study identified a further important mode of action for this intriguing dietary component by showing the distinct link between mitochondrial activity regulation and cell cycle regulation by 3,3′-diindolylmethane that might be exploited for the therapeutic development.

Acknowledgments

Received 11/21/2005; revised 1/20/2006; accepted 2/27/2006.

Grant support: Department of Defense, Army Breast Cancer Research Program grant DAMDI7-96-1-6149 and NIH grants CA69056 and CA102360.

The costs of publication of this article were defrayed in part by the payment of page charges. This article must therefore be hereby marked *advertisement* in accordance with 18 U.S.C. Section 1734 solely to indicate this fact.

References

1. Wortelboer HM, de Kruif CA, van Iersel AA, et al. Acid reaction products of indole-3-carbinol and their effects on cytochrome *P*450 and phase II enzymes in rat and monkey hepatocytes. Biochem Pharmacol 1992;43:1439–47.
2. De Kruif CA, Marsman JW, Venekamp JC, et al. Structure elucidation of acid reaction products of indole-3-carbinol: detection *in vivo* and enzyme induction *in vitro*. Chem Biol Interact 1991;80:303–15.
3. Chen I, McDougal A, Wang F, et al. Aryl hydrocarbon receptor-mediated antiestrogenic and antitumorigenic activity of diindolylmethane. Carcinogenesis 1998;19:1631–9.
4. Chang X, Tou JC, Hong C, et al. 3,3′-Diindolylmethane inhibits angiogenesis and the growth of transplantable human breast carcinoma in athymic mice. Carcinogenesis 2005;26:771–8.
5. Wiatrak BJ. Overview of recurrent respiratory papillomatosis. Curr Opin Otolaryngol Head Neck Surg 2003;11:433–41.
6. Sarkar FH, Li Y. Indole-3-carbinol and prostate cancer. J Nutr 2004;134:3493–8S.
7. Nachshon-Kedmi M, Fares FA, Yannai S. Therapeutic activity of 3,3′-diindolylmethane on prostate cancer in an *in vivo* model. Prostate 2004;61:153–60.
8. Hong C, Kim HA, Firestone GL, et al. 3,3′-Diindolylmethane (DIM) induces a G(1) cell cycle arrest in human breast cancer cells that is accompanied by Sp1-mediated activation of p21(WAF1/CIP1) expression. Carcinogenesis 2002;23:1297–305.
9. Hong C, Firestone GL, Bjeldanes LF. Bcl-2 family-mediated apoptotic effects of 3,3′-diindolylmethane (DIM) in human breast cancer cells. Biochem Pharmacol 2002;63:1085–97.
10. Gartel AL, Serfas MS, Tyner AL. p21-negative regulator of the cell cycle. Proc Soc Exp Biol Med 1996;213:138–49.
11. Xue L, Firestone GL, Bjeldanes LF. DIM stimulates IFNgamma gene expression in human breast cancer cells via the specific activation of JNK and p38 pathways. Oncogene 2005;24:2343–53.
12. Johnson GL, Lapadat R. Mitogen-activated protein kinase pathways mediated by ERK, JNK, and p38 protein kinases. Science 2002;298:1911–2.
13. Shen G, Xu C, Chen C, et al. p53-independent G(1) cell cycle arrest of human colon carcinoma cells HT-29 by sulforaphane is associated with induction of p21(CIP1) and inhibition of expression of cyclin D1. Cancer Chemother Pharmacol 2006;57:317–27.
14. Russo T, Zambrano N, Esposito F, et al. p53-independent pathway for activation of WAF1/CIP1 expression following oxidative stress. J Biol Chem 1995;270:29386–91.
15. Chandel NS, Schumacker PT. Cells depleted of mitochondrial DNA (rho0) yield insight into physiological mechanisms. FEBS Lett 1999;454:173–6.
16. Vaquero EC, Edderkaoui M, Pandol SJ, et al. Reactive oxygen species produced by NAD(P)H oxidase inhibit apoptosis in pancreatic cancer cells. J Biol Chem 2004;279:34643–54.
17. Mattiasson G. Analysis of mitochondrial generation and release of reactive oxygen species. Cytometry A 2004;62:89–96.
18. Zheng J, Ramirez VD. Piceatannol a stilbene phytochemical inhibits mitochondrial F0F1-ATPase activity by targeting the F1 complex. Biochem Biophys Res Commun 1999;261:499–503.
19. Kim R, Emi M, Tanabe K. Caspase-dependent and -independent cell death pathways after DNA damage. Oncol Rep 2005;14:595–9.
20. Kalbacova M, Vrbacky M, Drahota Z, et al. Comparison of the effect of mitochondrial inhibitors on mitochondrial membrane potential in two different cell lines using flow cytometry and spectrofluorometry. Cytometry A 2003;52:110–6.
21. Rottenberg H, Wu S. Quantitative assay by flow cytometry of the mitochondrial membrane potential in intact cells. Biochim Biophys Acta 1998;1404:393–404.
22. Boyer PD. The ATP synthase: a splendid molecular machine. Annu Rev Biochem 1997;66:717–49.
23. Aft RL, Zhang FW, Gius D. Evaluation of 2-deoxy-D-glucose as a chemotherapeutic agent: mechanism of cell death. Br J Cancer 2002;87:805–12.
24. Boonstra J, Post JA. Molecular events associated with reactive oxygen species and cell cycle progression in mammalian cells. Gene 2004;337:1–13.
25. Mattiazzi M, Vijayvergiya C, Gajewski CD, et al. The mtDNA T8993G (NARP) mutation results in an impairment of oxidative phosphorylation that can be improved by antioxidants. Hum Mol Genet 2004;13:869–79.
26. Chen Q, Vazquez EJ, Moghaddas S, et al. Production of reactive oxygen species by mitochondria: central role of complex III. J Biol Chem 2003;278:36027–31.
27. Turrens JF, Boveris A. Generation of superoxide anion by the NADH dehydrogenase of bovine heart mitochondria. Biochem J 1980;191:421–7.
28. Chang L, Karin M. Mammalian MAP kinase signalling cascades. Nature 2001;410:37–40.
29. Adler V, Yin Z, Fuchs SY, et al. Regulation of JNK signaling by GSTp. EMBO J 1999;18:1321–34.
30. Liu H, Nishitoh H, Ichijo H, et al. Activation of apoptosis signal-regulating kinase 1 (ASK1) by tumor necrosis factor receptor-associated factor 2 requires prior dissociation of the ASK1 inhibitor thioredoxin. Mol Cell Biol 2000;20:2198–208.
31. Saitoh M, Nishitoh H, Fujii M, et al. Mammalian thioredoxin is a direct inhibitor of apoptosis signal-regulating kinase (ASK) 1. EMBO J 1998;17:2596–606.
32. Salomon AR, Voehringer DW, Herzenberg LA, et al. Apoptolidin a selective cytotoxic agent is an inhibitor of F0F1-ATPase. Chem Biol 2001;8:71–80.
33. Izyumov DS, Avetisyan AV, Pletjushkina OY, et al. "Wages of fear": transient threefold decrease in intracellular ATP level imposes apoptosis. Biochim Biophys Acta 2004;1658:141–7.
34. Gemin A, Sweet S, Preston TJ, et al. Regulation of the cell cycle in response to inhibition of mitochondrial generated energy. Biochem Biophys Res Commun 2005;332:1122–32.
35. Armstrong JS, Hornung B, Lecane P, et al. Rotenone-induced G_2-M cell cycle arrest and apoptosis in a human B lymphoma cell line PW. Biochem Biophys Res Commun 2001;289:973–8.
36. King MA. Antimycin A-induced killing of HL-60 cells: apoptosis initiated from within mitochondria does not necessarily proceed via caspase 9. Cytometry A 2005;63:69–76.
37. Rancourt RC, Keng PC, Helt CE, et al. The role of p21(CIP1/WAF1) in growth of epithelial cells exposed to hyperoxia. Am J Physiol Lung Cell Mol Physiol 2001;280:L617–26.
38. Barnouin K, Dubuisson ML, Child ES, et al. H2O2 induces a transient multi-phase cell cycle arrest in mouse fibroblasts through modulating

Downloaded from cancerres.aacrjournals.org on March 25, 2019. © 2006 American Association for Cancer Research.

cyclin D and p21Cip1 expression. J Biol Chem 2002; 277:13761–70.
39. Engel RH, Evens AM. Oxidative stress and apoptosis: a new treatment paradigm in cancer. Front Biosci 2006;11:300–12.
40. O'Reilly MA. Redox activation of p21Cip1/WAF1/Sdi1: a multifunctional regulator of cell survival and death. Antioxid Redox Signal 2005;7:108–18.
41. Hainaut P, Milner J. Redox modulation of p53 conformation and sequence-specific DNA binding *in vitro*. Cancer Res 1993;53:4469–73.
42. Esposito F, Cuccovillo F, Vanoni M, et al. Redox-mediated regulation of p21(waf1/cip1) expression involves a post-transcriptional mechanism and activation of the mitogen-activated protein kinase pathway. Eur J Biochem 1997;245:730–7.
43. Kardassis D, Papakosta P, Pardali K, et al. c-Jun transactivates the promoter of the human p21(WAF1/Cip1) gene by acting as a superactivator of the ubiquitous transcription factor Sp1. J Biol Chem 1999; 274:29572–81.
44. Banki K, Hutter E, Gonchoroff NJ, et al. Elevation of mitochondrial transmembrane potential and reactive oxygen intermediate levels are early events and occur independently from activation of caspases in Fas signaling. J Immunol 1999;162: 1466–79.
45. Ly JD, Grubb DR, Lawen A. The mitochondrial membrane potential (deltapsi(m)) in apoptosis;an update. Apoptosis 2003;8:115–28.
46. Gartel AL, Tyner AL. The role of the cyclin-dependent kinase inhibitor p21 in apoptosis. Mol Cancer Ther 2002; 1:639–49.

Downloaded from cancerres.aacrjournals.org on March 25, 2019. © 2006 American Association for Cancer Research.

AACR American Association for Cancer Research

Cancer Research

The Journal of Cancer Research (1916–1930) | The American Journal of Cancer (1931–1940)

3,3′-Diindolylmethane Is a Novel Mitochondrial H^+-ATP Synthase Inhibitor that Can Induce $p21^{Cip1/Waf1}$ Expression by Induction of Oxidative Stress in Human Breast Cancer Cells

Yixuan Gong, Heesook Sohn, Ling Xue, et al.

Cancer Res 2006;66:4880-4887.

Updated version	Access the most recent version of this article at: http://cancerres.aacrjournals.org/content/66/9/4880

Cited articles	This article cites 46 articles, 13 of which you can access for free at: http://cancerres.aacrjournals.org/content/66/9/4880.full#ref-list-1
Citing articles	This article has been cited by 8 HighWire-hosted articles. Access the articles at: http://cancerres.aacrjournals.org/content/66/9/4880.full#related-urls

E-mail alerts	Sign up to receive free email-alerts related to this article or journal.
Reprints and Subscriptions	To order reprints of this article or to subscribe to the journal, contact the AACR Publications Department at pubs@aacr.org.
Permissions	To request permission to re-use all or part of this article, use this link http://cancerres.aacrjournals.org/content/66/9/4880. Click on "Request Permissions" which will take you to the Copyright Clearance Center's (CCC) Rightslink site.

Downloaded from cancerres.aacrjournals.org on March 25, 2019. © 2006 American Association for Cancer Research.